INTERNAL PRESSURE DEVELOPMENT AND DEFORMATION DURING SUPERCRITICAL FLUID IMPREGNATION OF SELECTED WOOD-BASED MATERIALS

Georg Oberdorfer†
Former Visiting Scientist
Holzforschung Austria
Franz Grill-Straße 7
1030 Wien, Austria

Robert J. Leichti
Associate Professor

and

Jeffrey J. Morrell†
Professor
Department of Wood Science and Engineering
Oregon State University
Corvallis, OR 97331

(Received December 2004)

ABSTRACT

The effect of supercritical carbon dioxide impregnation on pressure development was assessed on oriented strandboard (OSB), medium density fiberboard (MDF), laminated veneer lumber (LVL), and solid-sawn Douglas-fir heartwood lumber. Pressure differences between the surface and the interior were relatively small with MDF and OSB, owing to the presence of numerous pathways for fluid flow. Pressure differences tended to be higher in LVL and solid wood, but were still below the levels necessary for inducing material damage, except when flow directions were restricted and pressure was rapidly applied. The results indicate that supercritical fluid (SCF) impregnation is suitable for most composites, although care must be taken to limit pressure changes in situations where flow is restricted.

Keywords: Supercritical fluids, oriented strandboard, medium density fiberboard, laminated veneer lumber, internal pressure.

INTRODUCTION

The growing use of wood-based composites in construction has greatly increased the risk that these materials will be used under conditions that are conducive to decay. Although the presence of adhesives in some composites increases decay resistance compared with solid wood of the same species, these materials are generally not markedly more decay resistant. Supplemental treatment with water-based preservatives is possible with some materials such as plywood, laminated timbers, or parallel strand lumber, but it can lead to unacceptable, permanent expansion and deformation on composites such as medium density fiberboard (MDF), particleboard, or oriented strandboard (OSB). Acceptable treatments can be achieved with oil-based preservatives, but residual solvents in the panels create handling difficulties and odor issues. An alternative approach is to add preservative to the finish prior to pressing, but many composite manufacturers object to the use of pesticides in their plants.

† Member of SWST.

The continued expansion of markets for wood-based composites into decay prone applications will require the development of technologies for protecting against decay without adversely affecting panel properties. One strategy for impregnating panels is to use supercritical fluids (SCFs) as carriers for biocides. Supercritical fluids are materials that have been heated and pressurized beyond their critical temperature and pressure (Clifford 1998). They have diffusivities that approach those of gases, allowing them to readily penetrate porous materials (Debenedetti and Reid 1986). Many SCFs also have solvating properties that approach those of liquids. Although these materials have been explored for a variety of extraction processes (Beer and Peter 1985; Calimli and Olcay 1978; Chou 1987; Eller and King 2000; Fremont 1981; Funazukuri 2000; Hendriksen 2000; Kiran 1995; Larsen et al. 1992; Levien et al. 1994; Morita et al. 1995; Ohira et al. 1994; Ping 1997; Ritter and Campbell 1986; Ruddick and Cui 1995; Sahle Demessie et al. 1997; Sunol 1991, 1992; Terauchi et al. 1993) far less is known about their use for deposition of materials in a wood matrix (Acda et al. 2001; Bertucco et al. 1994; Brandt et al. 1994; Kayihan 1992; Morrell and Levien 2000; Morrell et al. 1993; Smith et al. 1993).

Acda et al. (1997a, b) used supercritical carbon dioxide (SC-CO_2) to deliver fungitoxic levels of tebuconazole into plywood, particleboard, MDF, and OSB without adversely affecting panel properties. However, they noted a wide variation in retention levels under similar process conditions, as well as some densification of the panels. The SCF-impregnation process is especially sensitive to pressure and temperature; failure to control these variables can lead to substantial differences in deposition. Unfortunately, little information exists on *in situ* pressure, temperature, or dimensional changes during SCF impregnation of wood-based materials. This information will be critical for developing reproducible SCF impregnation processes for the wide of array of wood products.

The objective of this research was to conduct a carefully planned and controlled experiment where wood-based composites were treated with SC-CO_2. The purpose was to monitor and evaluate the effects of the SCF treatment on the dimensional and residual properties of sawn wood, laminated veneer lumber (LVL), OSB, and MDF.

MATERIALS AND METHODS

Four materials were selected for study: sawn coastal Douglas-fir (*Pseudotsuga menziesii* (Mirb.) Franco) heartwood lumber, aspen OSB, and two thicknesses of softwood MDF. The LVL was composed of 9 plys of 2.54-mm-thick Douglas-fir veneer cut into 20- or 30- by 30- by 60-mm-long specimens. All specimens were conditioned to constant weight at 65% relative humidity and 20°C prior to treatment.

In order to simulate larger panels and limit flow paths, specific flow paths were restricted by the application of two coats of a two-part epoxy sealant. OSB panels required three coats of epoxy for an effective seal.

Treatment parameters

All treatments were performed using a supercritical fluid pilot plant (Fig. 1). Although the treatment fluid in a SCF-impregnation process will most likely comprise CO_2, a co-solvent, and the solute, CO_2 alone was used in our trials and

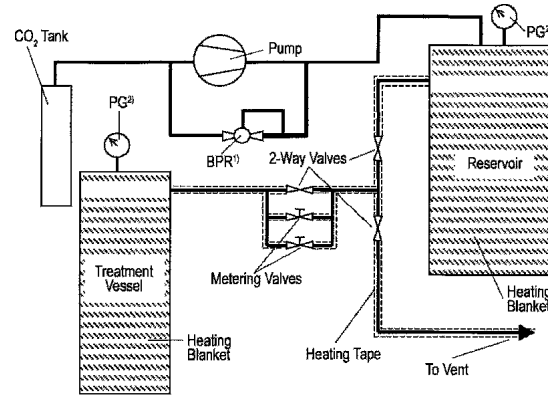

FIG. 1. Components of the SCF impregnation plant used in the experimental work.

TABLE 1. *Process parameters employed during SCF treatment.*

Treatment pressure Pmax	Treatment temperature	Treatment period @ Pmax	Pressurization rate	Venting rate
9 MPa	40°C (313.02 K)	10 min	1.03 MPa/min	1.03 MPa/min
			1.79 MPa/min	1.79 MPa/min
			5.86 MPa/min	5.86 MPa/min

was assumed to closely mimic the conditions encountered during treatments with a ternary mixture. We used three different pressurization and venting rates and each rate was repeated for four to five samples (Table 1). The targeted treatment pressure was well above the respective critical value for CO_2 (P_c: 7.38 MPa), since impregnation tends to be more efficient at higher pressures (Sahle Demessie 1994; Acda 1997b; Sahle Demessie et al. 1998). The treatment period was kept short to avoid excessive softening and successive failure of the end sealant. With the exception of a few treatments, the treatment period of 10 min provided sufficient time for pressure equilibration in the specimens.

Before the start of a treatment run, the tubing, valves, treatment vessel, and the reservoir were heated to the treatment temperature (40°C) using heating blankets and heating tape. This reduced the effects of rapid cooling during the expansion of the gas on the steady function of the metering valves. Standard grade CO_2 (Industrial Welding Supply, Albany, OR) was pumped from a tank into the reservoir until the pressure inside the latter reached approximately 31 MPa. About 1 h before the start of the treatment, the specimens were placed in the treatment vessel to allow them to reach the target temperature. Thicker specimens (31-mm MDF, LVL, and Douglas-fir) were preheated to around 35°C just prior to placement in the treatment vessel. The system was flushed with CO_2 before any initial heating period. Upon completion of these preparations, the data collection system was initialized and the treatment vessel was pressurized.

Vessel pressure was steadily increased by manually controlling the flow of CO_2 from the reservoir through two micrometering valves into the treatment vessel. Although heating the valves helped to reduce the negative effect of the rapid temperature drop, this effect and the resulting inconsistent flow could not be totally avoided. Furthermore rapid increases in density near the critical region made it more difficult to maintain a linear pressure increase (Fig. 2). Pressure drop was compensated for by initially pressurizing the treatment vessel to around 9.2 MPa, since at the end of the pressurization the temperature of the SC-CO_2 tended to be slightly higher than 40 C (Fig. 2).

Depressurization was controlled by allowing the CO_2 to flow through the metering valves to a vent. Fresh CO_2 gas was used for each treatment, since the pilot plant configuration did not accommodate collection and recycling.

Data acquisition

The data acquisition system consisted of a Campbell CR 7X datalogger (Campbell Scientific Inc. Logan, UT), a Campbell SC 32A interface, and a laptop computer for data collection and short-term data storage. Given the num-

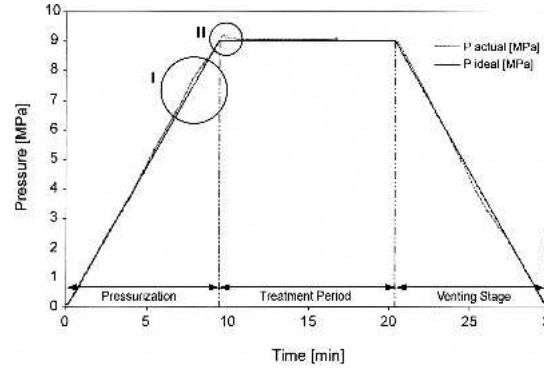

FIG. 2. Pressure development inside the treatment vessel during an ideal and real treatment run at pressurization and venting rates of 1.03 MPa/min showing deviations from desired rates I and II.

ber of operations the datalogger had to carry out at the desired resolution, 1.5-s intervals were determined to be the shortest practical intervals for data collection. Data were collected using Term Ver3.1 (Campbell Scientific Inc., Logan UT). ProComm (Datastorm Technologies Inc., Columbia, MO) was used for the experiments on MDF, LVL, and Douglas-fir.

Continuous pressure measurements were made inside the samples by inserting a pressure probe into a sample (Fig. 3). Lowery (1971; 1972) used Teflon™ capillary tubing to measure vapor pressure in samples of Engelmann spruce during drying. A similar approach was also used to determine pressure inside wood samples during impregnation (Resch and Arganbright 1970; Orfila and Hosli 1985; Cobham and Vinden 1995; Schneider and Morrell 1997; Schneider 1999) and vapor pressure inside wood composite materials during pressing (Kamke and Casey 1988; Zavala and Humphrey 1996; Zavala 1990). The latter two studies further reduced the dead volume in their thin stainless steel pressure probes by using silicone oil to improve pressure change transfer to the diaphragm of the pressure transducer.

The probes were 80 mm long and were cut from stainless steel tubing (High Pressure Equipment Co., Erie, PA) (1.59 mm o.d., 0.15 mm i.d.). The small inner diameter helped to minimize dead volume. A two-stage hole, with holes 3.2 mm and 1.6 mm in diameter, was drilled into the sample (Fig. 3). The probe was inserted to the desired depth and the space around the probe was filled by injecting heated epoxy with a syringe. Heating the resin lowered viscosity, allowing the resin to more evenly fill the spaces around the probe. In addition, the steel surfaces of the pressure probes were lightly abraded with sandpaper to enhance epoxy and resin bonding. A polyurethane sleeve was placed around the probe 3.2 mm in to prevent epoxy from reaching the tip and thus hindering flow into the probe. The 1.6-mm hole diameter was also extended slightly beyond the length of the probe to create a small void space that helped to prevent local differences in permeability from affecting the consistency of the pressure measurements.

The pressure samples were suspended inside the treatment vessel from the vessel cap using a stainless steel cage that minimized specimen movement during treatment (Fig. 4). The pressure signal was transferred from the probes inside the samples to the transducers on the outside of the treatment vessel via stainless steel tubing fed through the plug of the vessel. The first section of the tubing had the same specifications as the tubing used for the pressure probes

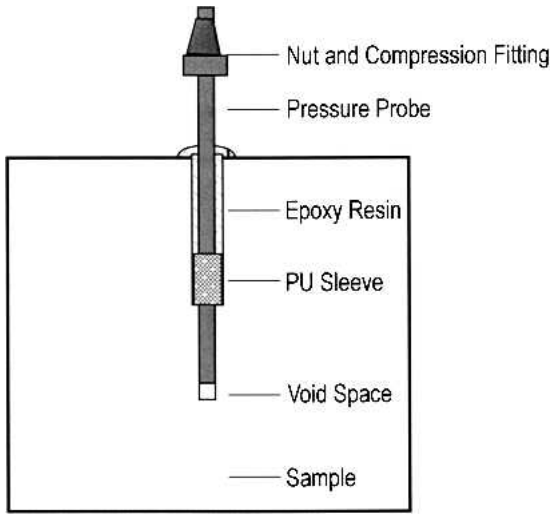

FIG. 3. Schematic of the probe used to measure pressure inside of samples during SCF impregnation.

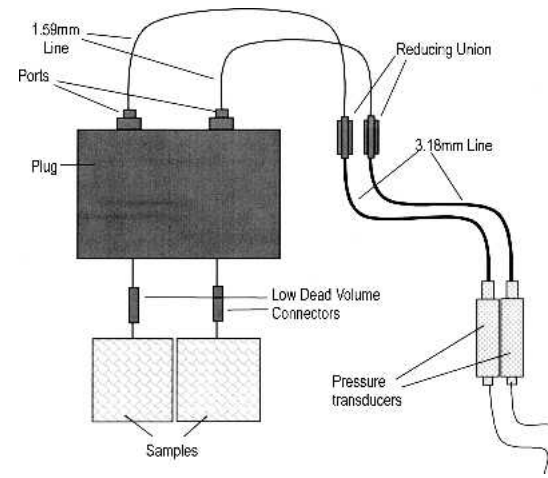

FIG. 4. Schematic of sample installation and measurement set-up in the treatment vessel.

and used as the transfer medium. The tube was connected to a 3.18-mm-diameter tubing filled with Dot 5 silicone oil (Johnsen, Dallas, TX) to transfer the pressure from the microbore tubing to the Omega PX 520–5K GI pressure transducers (Omega Engineering Co., Stamford, CT). The electrical output signal from the pressure transducers was processed by the Campbell datalogger and stored on a laptop computer. Pressure was also simultaneously displayed on the control panel of the SCF impregnation equipment. Each pressure sample was visually inspected after treatment to detect evidence of damage. Each sample was then cut in half to allow inspection of probe installation. The pressure probes were then removed from the sample and the adhering epoxy resin was sanded off so the probes could be reused.

Temperature measurement

Temperatures on the surface and inside the wood were measured using ANSI Type K thermocouples (TT-K-36 by Omega Engineering Inc., Stamford, CT). Treatment fluid temperatures inside the vessel were measured using thicker ANSI Type K thermocouple (TT-K-24). The same material was used to provide all the connections between the thermocouples and the datalogger by routing the wires through a feedthrough (Connex Buffalo Technologies, Buffalo, NJ) installed in the plug of the vessel. The "Liquid Crystal Polymer" housing of the miniature connectors (HMPW-K-MF, Omega Engineering Inc., Stamford, CT) was not noticeably swollen or otherwise affected by SC-CO_2.

One thermocouple was epoxied into a 1.02-mm-diameter predrilled hole close to center in each OSB and MDF specimen (Table 2). Two thermocouples were installed inside LVL and Douglas-fir specimens, one at the center of the specimen and one 10 mm from the open, unsealed edge and at equal distances from the sealed sides. One thermocouple was glued to the surface of each specimen. The thermocouple wire was strong enough to act as a support for the specimens, which were suspended approximately 100 cm below the vessel plug. Thermocouple output was processed by the Campbell datalogger using its standard program setting for Type K thermocouples.

RESULTS AND DISCUSSION

Pressurization

Internal pressure in OSB and MDF during pressurization at three different rates showed that gaseous as well as SC-CO_2 rapidly penetrated the respective material matrices (Figs. 5 and 6). No treatment defects were observed in any of the pressure samples. Although the variability of the measured pressure gradients on a

TABLE 2. *Specifications of samples used to measure pressure development during SCF treatment.*

Material	Avg. density (kg/m^3)[a]	Replicates (pressure)	Replicates (temp)	Thickness (mm)	Width (mm)	Length (mm)	Flow path (mm)[b]
OSB	643.2 (42.5)	30	—	10.9	60	60	20 (x), 5 (v)
		—	30	10.9	60	60	30 (x), 5 (v)
		30	—	10.9	60	60	40 (x), 5 (v)
		6	—	10.9	60	60	5 (v)
MDF	804.2 (22.1)	36	18	17	60	60	7 (v)
	769.8 (8.1)	12	6	31	60	60	14 (v)
LVL	583.0 (19.3)	24	12	30	60	60	30 (p)
		19	12	30	60	60	30 (v)
		5	—	30	20	60	10 (v)
Douglas-fir	596.3 (71.9)	7	3	30	60	60	30 (R)
		7	4	30	60	60	30 (T)

[a] Density after equilibration at 20°C and 65% RH. Values in parentheses represent one standard deviation.

[b] The letters in parentheses give the designated flow path in the samples: (x) horizontal, parallel to fiber or strand orientation; (v) vertical, perpendicular to plane of composite panel or plies in LVL; (p) vertical, parallel to plane of plies in LVL; (R) radial in solid wood; (T) tangential in solid wood.

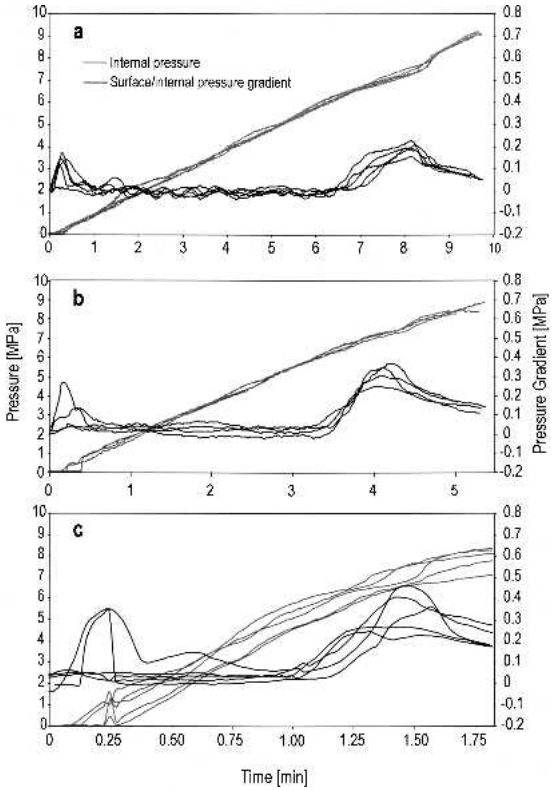

FIG. 5. Development of internal pressure and pressure gradients in OSB during pressurization at (a) 1.03, (b) 1.79, or (c) 5.86 MPa/min. Each line represents a single embedded sensor response.

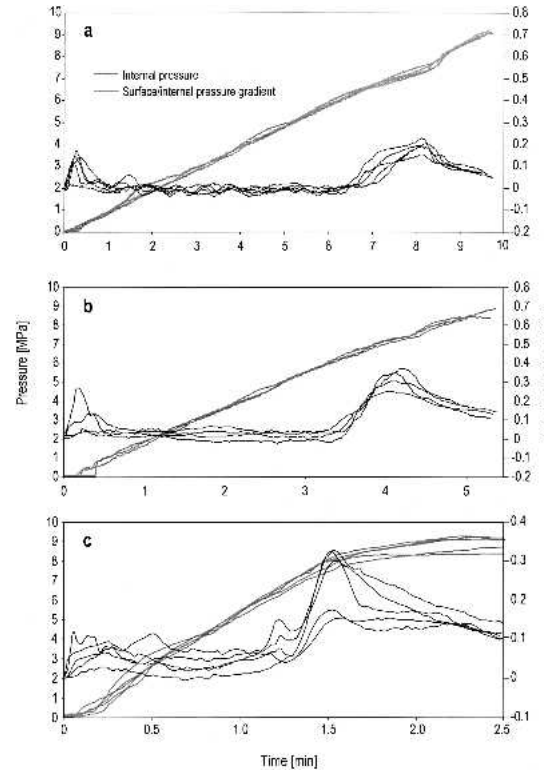

FIG. 6. Development of internal pressure and pressure gradients in 17-mm-thick MDF during pressurization at (a) 1.03, (b) 1.79, or (c) 5.86 MPa/min. Each line represents response from a single pressure sensor.

percentage basis was high—especially at the lower pressurization rates—neither OSB nor MDF specimens were exposed to excessive compressive stresses as the pressure was raised from 0.1 MPa (atmospheric pressure) to 9 MPa. Maximum pressure gradients were measured between 0.1 and 1 MPa and near the phase transition to the supercritical region. Flow conditions seemed to stabilize again above 8.0–8.5 MPa. Increased pressure gradients coincided with a rapid and substantial increase in calculated CO_2 density and solvating strength near the critical pressure (Fig. 7). Rapid density increase under constant volumetric flow should be counteracted by higher pressure gradients and increased fluid flow velocity. Mass flow above the phase transition region declined as fluid density increased more slowly with increasing pressure (Fig. 8).

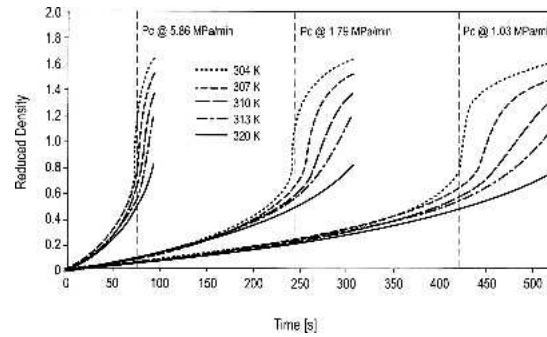

FIG. 7. Development of reduced density ($/_c$) at 5 temperatures during pressurization to 9 MPa at rates of 1.03, 1.79, and 5.86 MPa/min.

This should lower pressure gradients as shown in the experimental data. The small increase in fluid viscosity will also result in a higher pressure gradient. Darcy's law is strictly applicable

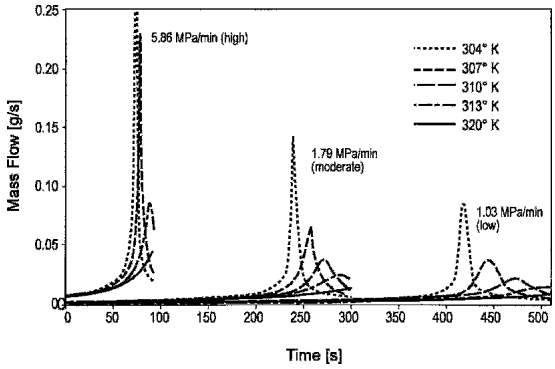

FIG. 8. Relationship between calculated mass flow into an OSB sample and pressurization rate (1.03, 1.79, or 5.86 MPa/min.) and temperature (304, 307, 310, or 320°K).

to single-phase flow only. Permeability is no longer totally dependent on the substrate if two or more phases are present and the available flow area must be divided by introducing a multiplication factor referred to as relative permeability (Hawes 1996). This effect may be negligible, however, since it may not occur in a supercritical fluid and since the single-phase model successfully predicts supercritical fluid flow through a porous material. Furthermore, the stability of permeability during supercritical fluid flow through wood is unknown. Many low-molecular-weight wood constituents are soluble in SC-CO_2 and reports indicate that such substances are indeed dissolved during SCF treatments (Ritter and Campbell 1991; Sahle Demessie et al. 1995). Finally, interactions between the SC-CO_2 and the silicone oil used in the section of the tubing connecting the pressure probes to the transducers may influence the accuracy of the pressure measurements.

Pressure gradients over a pressure range of 3.0 to 6.5 MPa were similar during pressurization at all three rates although variability increased at the highest pressure rate. Average pressure gradients in MDF and OSB did not exceed 0.1 MPa at any of the three pressurization rates (Table 3). Measurements at the two lower pressurization rates were strongly influenced by electronic noise in the data acquisition system. This interference exceeded any slight differences between the MDF sample configurations despite the longer flow paths in the 30-mm-thick specimens and their slightly lower permeability.

Development of internal pressure in LVL was strongly affected by the designated flow directions. No excessive pressure gradients developed when CO_2 flowed parallel to the grain direction (Fig. 9). Six specimens developed very fine cracks in the epoxy sealants, which may have resulted from pressure build-up underneath the sealant or by small deformations in the samples. Wood was not visibly damaged on any of the specimens. Gaps, knots, and finger-joints created pathways for parallel flow in LVL. Veneer permeability was further increased by the

TABLE 3. *Average pressure gradients in OSB, MDF, and LVL during pressurization at 1.03, 1.79, or 5.86 MPa/min.*

Material	Pressurization rates (MPa/min)	Average pressure gradient (MPa)[a]	Standard deviation (MPa)[a]	Number of samples/runs
OSB	1.03	0.016	0.025	10/5
	1.79	0.012	0.016	5/4
	5.86	0.097	0.084	7/5
MDF[b]	1.03	0.035	0.028	8/4
	1.03 (17 mm)	0.042	0.030	6/3
	1.79	0.056	0.026	8/4
	1.79 (17 mm)	0.055	0.030	6/3
	5.86	0.098	0.058	8/5
	5.86 (17 mm)	0.078	0.063	7/4
LVL (p)	1.03	0.242	0.024	4/4
	1.79	0.282	0.108	3/3
	5.86	0.507	0.560	3/3

[a] Average and standard deviations of pressure gradients measured between 3.0–6.5 MPa.
[b] Values for averages and standard deviations calculated from a combination of 17- and 31-mm thick samples (PL, PM and PH) and from 17-mm samples only.

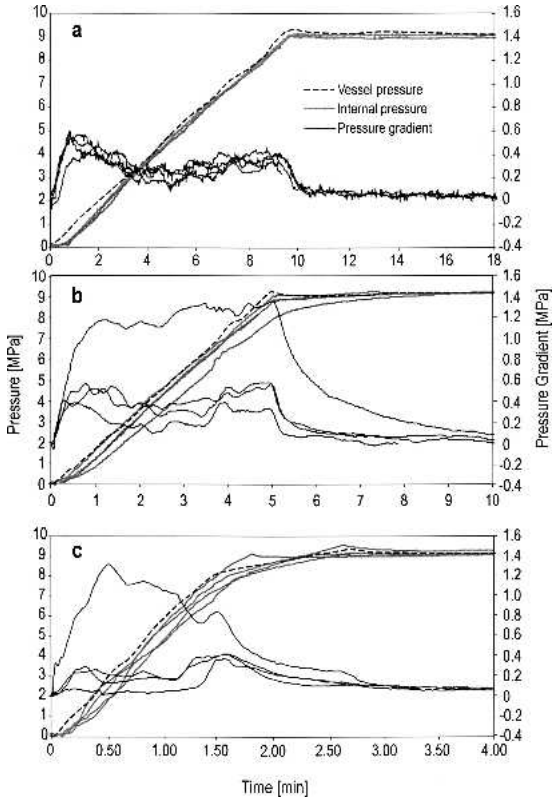

FIG. 9. Development of internal pressure and pressure gradients in LVL with flow restricted to the parallel direction during pressurization at (a) 1.03, (b) 1.79, or (c) 5.86 MPa/min. Each line represents a single pressure transducer. P vessel represents vessel pressure during one treatment.

presence of lathe-checks that were clearly visible to the naked eye.

As with MDF and OSB, pressure gradients peaked during initial pressurization and phase transition; however, peaks were not as distinct in LVL. Although average pressure gradients increased at higher pressurization rates, reflecting two runs with exceptionally high pressure gradients (Fig. 9), the influence of pressurization rate was not as strong as expected (Table 3). Indeed, internal pressure response during pressurization at 5.86 MPa/min seemed to be more rapid than at lower rates. The reason for this observation remains unclear. Gaseous and supercritical CO_2 flow patterns through materials with more diverse flow paths should differ from the assumed Darcyan flow regime. The development of pressure gradients in Douglas-fir heartwood showed a much stronger dependence on the pressurization rate (Fig. 10). Pressure gradients in Douglas-fir samples during penetration by tangential flow were around 5–10 times higher than in LVL. These differences illustrate the importance of alternative flow paths during high pressure impregnation of semi-porous materials such as wood.

CO_2 flow in the vertical direction was strongly influenced by the gluelines (Fig. 11). The majority of the LVL samples were nearly impenetrable across the gluelines. Consequently two specimens experienced slight crushing while the other specimens were severely crushed, particularly in plies with a high per-

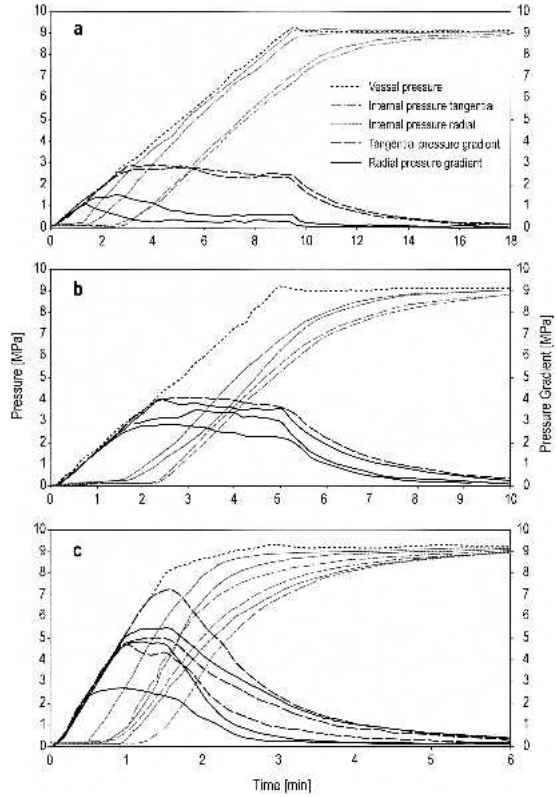

FIG. 10. Development of internal pressure and pressure gradients in Douglas-fir heartwood with flow restricted to the radial or tangential direction at pressurization rates of (a) 1.03, (b) 1.79, or (c) 5.86 MPa/min. Each line represents a single pressure transducer. P vessel represents the vessel pressure during one treatment. Lines with the same symbols represent similar wood orientations.

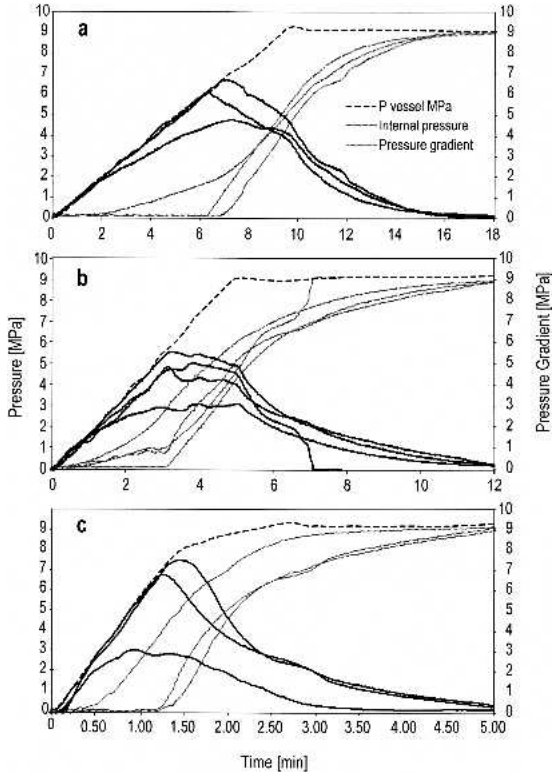

FIG. 11. Development of internal pressure and pressure gradients in LVL with flow restricted to the vertical direction during pressurization at (a) 1.03, (b) 1.79, or (c) 5.86 MPa/min. Each line represents a single pressure transducer. P vessel represents vessel pressure during one treatment.

centage of earlywood. Collapse occurred in most samples within 15 mm of the center, supporting the hypothesis that the stresses built up towards the center of the specimen. However, collapse sometimes occurred in plies closer to the surface and in one specimen where the flow path length was reduced to 1 cm. This suggests that the pressure drop varied between specimens and was strongly influenced by the position of individual gluelines, which formed a closed film between plies and retarded CO_2 flow. Specimen failure under the high compressive force opened cracks in the sealant for parallel flow that sharply reduced the pressure differential.

Maximum pressure gradients should therefore be regarded as a stronger indicator of compressive strength than permeability. Maximum pressure gradients ranged from 3.5 to 7.5 MPa. a range corresponding to the design values for compressive strength of LVL (2.8 to 4.2 Mpa) (USDA 1999). Exposing LVL samples with their parallel and longitudinal flow paths sealed led to steadily increasing internal pressures until failure in compression occurred (Fig. 12). Flow in the vertical direction in LVL samples translates into radial flow in the individual Douglas-fir veneers. Comparison between results from LVL samples and those from solid Douglas-fir samples showed that pressure gradients in LVL were up to 7 times higher. Because collapse occurred at very low pressurization rates, the increased pressure gradients with increasing pressing rates could not be observed in the same way in LVL as in Douglas-fir samples (Fig. 10).

Penetration in solid Douglas-fir specimens followed the assumed Darcyan flow model more closely than LVL. Pressure gradients increased markedly with increasing pressing rates. Pressure gradients in samples with radial flow paths rose proportionally with increased pressurization rates. Pressurizing the treatment vessel at 5.86 MPa/min produced collapse in two samples. Pressure gradients were much higher in the two samples with flow restricted to the tangential direction than in those with radial flow paths when samples were pressurized at 1.03 MPa/min. This effect was either reduced or inconsistent at pressurization rates of 1.79 and 5.86 MPa/min, respectively.

Radial permeability of solid wood should be enhanced by the rays resulting in lower pressure gradients. However, published permeability val-

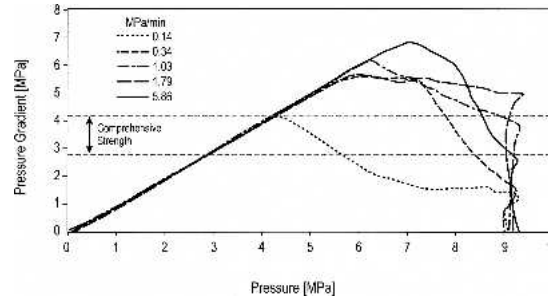

FIG. 12. Development of pressure gradients in LVL during pressurization at rates ranging from 0.14 to 5.86 MPa with flow restricted to the vertical direction. Dotted lines show the range of reported compressive strength for LVL.

ues for Douglas-fir heartwood are not consistently lower in the radial direction (Comstock 1970; Choong et al. 1972; Schneider 1999). Variability between individual specimens might contribute to the small differences in pressure gradients between samples with radial and tangential flow paths. Comparisons between LVL and Douglas-fir samples indicated that the penetration process and ultimately calculations of allowable pressurization rates were more complex in the laminated material.

Venting rate

Internal pressure in OSB and MDF samples decreased at rates similar to the respective ventilation rates (Figs. 13 and 14, respectively). Substantial pressure gradients were not encountered nor was visible damage observed on any specimens. Peaks in pressure gradients were observed during phase transition and towards the end of the ventilation. Increased pressure gradients in the region near the critical point probably occur for the same reasons described earlier. Maximum tension forces as a result of pressure gradients were exerted on the samples at the end of the venting stage.

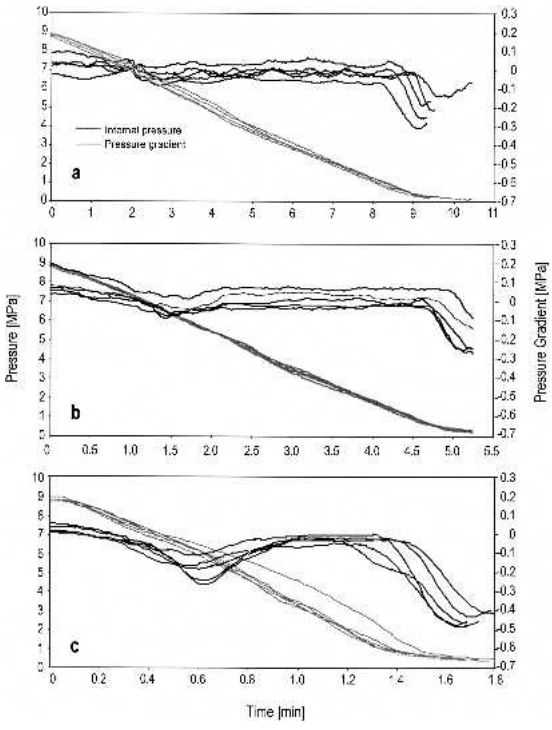

FIG. 13. Development of internal pressure and pressure gradients in OSB during venting at (a) 1.03, (b) 1.79, or (c) 5.86 MPa/min. Each line represents a single pressure transducer.

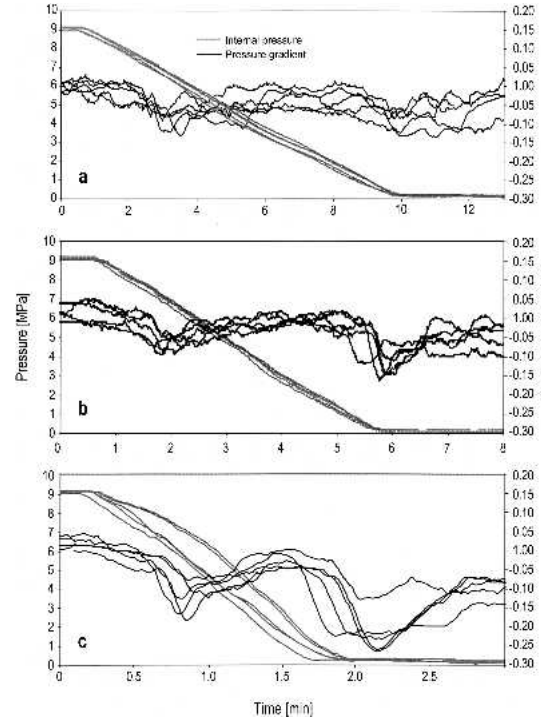

FIG. 14. Development of internal pressure and pressure gradients in 17-mm-thick MDF during ventilation at (a) 1.03, (b) 1.79, or (c) 5.86 MPa/min. Each line represents a single pressure transducer.

Schneider (1999) also encountered pressure gradients in refractory solid wood samples at the end of the venting stage; however, his gradients were much higher as were the time periods until pressure equilibrated. In our experiments, total pressure equilibration generally took less than 2 min. Pressure gradients between the vessel and panel interior were very small in the pressure range between 3.0 and 6.5 MPa at higher ventilation rates (Table 4); however, pressure gradients were more pronounced during the phase transition and the final pressure drop. A more rapid expansion of the fluid at higher venting

TABLE 4. *Average pressure gradients in OSB, MDF, and LVL during venting at 1.03, 1.79, and 5.86 MPa/min.*

Material	Pressurization rates (MPa/min)	Average pressure gradient (MPa)[a]	Standard deviation (MPa)[a]	Number of samples/runs
OSB	1.03	−0.019	0.059	10/5
	1.79			
	5.86	−0.053	0.032	10/5
MDF[b]	1.03	−0.071	0.035	8/4
	1.03 (17 mm)	−0.067	0.037	6/3
	1.79	−0.094	0.087	8/4
	1.79 (17 mm)	−0.100	0.095	6/3
	5.86	−0.110	0.040	7/7
	5.86 (17 mm)	−0.100	0.024	6/6
LVL (p)	1.03	−0.201	0.183	4/4
	1.79	−0.275	0.122	4/4
	5.86	−0.357	0.257	4/4
LVL (v)	1.03	−0.298	0.316	4/4
	1.79	−0.367	0.054	4/4
	5.86	−0.712	0.338	4/4

[a] Average and standard deviations of pressure gradients measured between 3.0–6.5 MPa.
[b] Values represent means and standard deviations for a combination of 17- and 31-mm thick samples and from 17-mm samples only.

rates brought about a more severe drop in temperature and fluid density near the critical region contributing to increased pressure gradients with increased venting rates. Pressure differences between OSB and MDF samples with different flow paths and flow path lengths were again negligible (Figs. 13 and 14).

Pressure gradients that developed during venting in LVL specimens with flow restricted to the parallel direction were comparable to those observed at similar pressurization rates, but there was no evidence of wood damage (Fig. 15). Small cracks in the epoxy on six specimens were regarded as qualitative indicators of pressure development underneath the resin or of slight deformation in the samples. Although higher pressure gradients were observed in several treatments near the critical region and near the end of the venting stage, these effects were less pronounced in LVL. Higher temperatures as a result of wood occupying more vessel volume during the LVL treatments may have limited density decreases and thus the development of pressure gradients (Fig. 7). LVL samples also tended to be less permeable than OSB and MDF as evidenced by the slower equilibration to atmospheric pressure at the end of the treatment. Pressure gradients in LVL with parallel flow paths were still several times lower than those

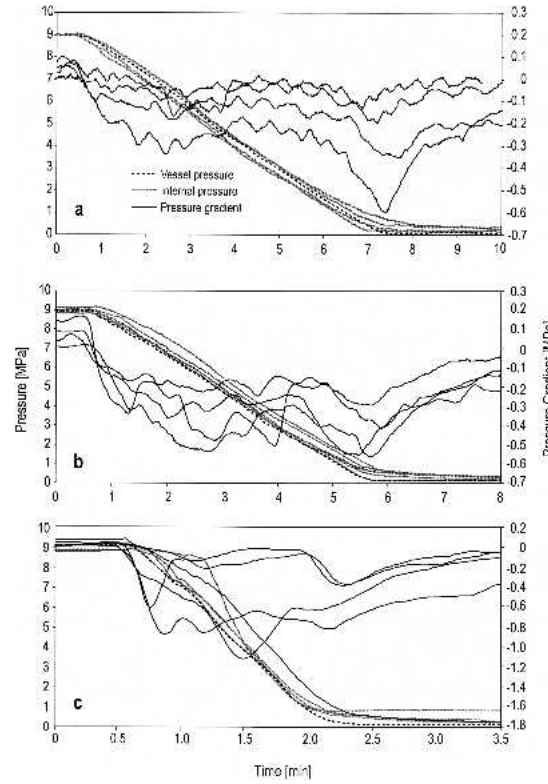

FIG. 15. Development of internal pressure and pressure gradients in LVL with flow restricted to the vertical direction during ventilation at (a) 1.03, (b) 1.79, or (c) 5.86 MPa/min. Each line represents a single pressure transducer. P vessel represents the vessel pressure during one treatment.

found with Douglas-fir samples opened to tangential flow (Fig. 16).

LVL samples open to vertical flow experienced limited flow (Fig. 15) and most were damaged during treatment. Therefore, the reported values more likely reflect penetration by parallel flow through cracks in the sealant rather than by true vertical flow. The results suggest that gluelines hindered flow to such an extent that even very slow pressure changes produced mechanical damage.

Pressure development in solid Douglas-fir samples indicated that the material had lower tangential permeability (Fig. 17). Ventilation at 1.03 or 1.79 MPa/min led to splitting of three samples with tangential flow paths. Maximum pressure gradients were observed at the end of venting, and final pressure equilibration often

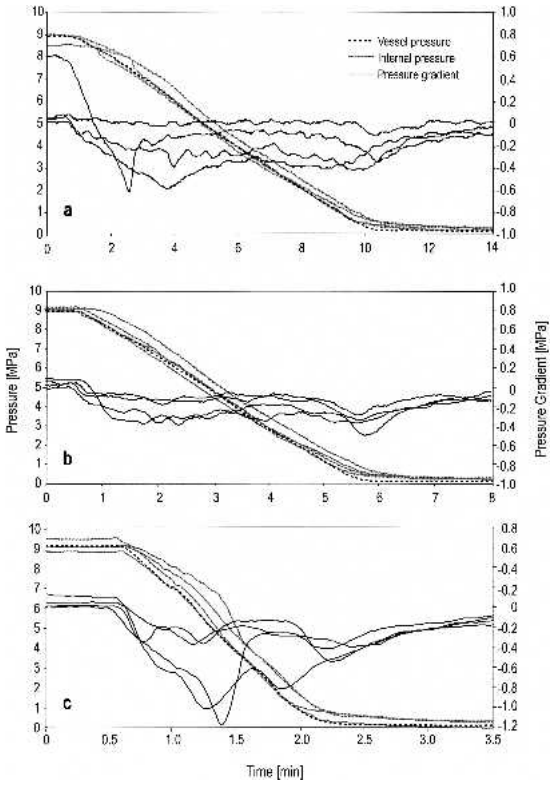

FIG. 16. Development of internal pressure and pressure gradients in LVL with flow restricted to the parallel direction during ventilation at (a) 1.03, (b) 1.79, or (c) 5.86 MPa/min. Each line represents a single pressure transducer. P vessel represents the vessel pressure during one treatment.

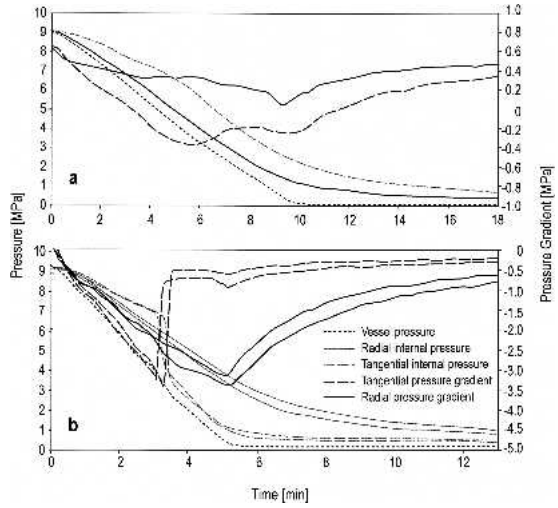

FIG. 17. Development of internal pressure and pressure gradients in Douglas-fir heartwood with flow restricted to the radial or tangential direction during ventilation at (a) 1.03 and (b) 1.79 MPa/min. Each line represents a single pressure transducer. P vessel represents the vessel pressure during one treatment. Lines with the same symbols represent similar wood orientations.

required more than 30 min after the vessel had returned to atmospheric pressure. Differences in tangential and radial permeability became very noticeable during the process. The assumed flow pattern was again reflected, to a high degree, by the increases in pressure gradients as venting rates increased from 1.03 to 1.79 MPa/min. Severe specimen damage limited data collection for Douglas-fir samples vented at 5.86 MPa/min.

Temperature measurements

Expansion of supercritical CO_2 from the reservoir into the treatment vessel during pressurization tended to lower the system temperature. Pressurization at higher rates led to faster, more severe temperature drops (Fig. 18). Temperature development during pressurization can be affected by heat conduction from heating devices to different components of the treatment plant. Although these devices could not prevent drops in temperature below the target value (40°C, 313K) during pressurization, they limited the extent of decline.

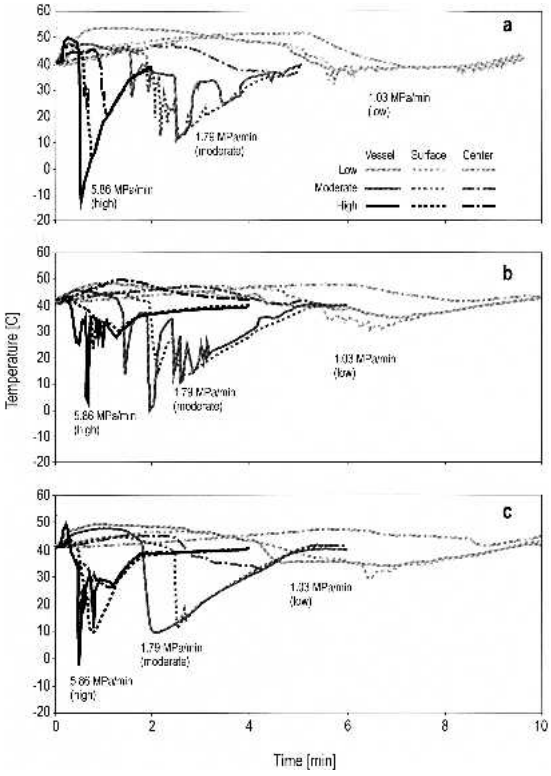

FIG. 18. Temperatures in the treatment vessel, on the surface and at the center of (a) OSB, (b) MDF, and (c) LVL samples during pressurization at 3 rates.

Temperature development at different locations in the treatment system varied substantially between individual treatment runs (Table 5). The reasons for these variations are unclear, since target temperature and initial temperature of the reservoir were constant for all treatments. Temperatures during pressurization at all three measurement locations in the vessel initially increased from 40°C up to 55°C then declined to levels on the saturation line corresponding to the pressure present in the system in all treatments at pressing rates at or above 1.79 MPa/min and in several treatments at 1.03 MPa/min. Energy released during condensation of gaseous CO_2 (latent heat) then increased temperature. Consequently, the temperature in the system was at or very near the critical value when the critical pressure was reached.

Although it is unclear how the presence of two physical states of CO_2 might affect treatment, solvent properties (density, solvating strength, viscosity, etc.) undergo their most dramatic changes near the critical region. For future applications of SCF treatments, these relationships must be considered when selecting target temperatures or process parameters that influence temperature. Failure to consider these influences will result in sub-critical conditions that introduce considerable variation to the process (Fig. 18).

Rates at which temperature changes occurred depended on the media surrounding the thermocouples (CO_2, CO_2/wood, or wood) and the rate of heat exchange between media. Convection fa-

TABLE 5. *Average temperature maxima and minima measured inside the treatment vessel, on the surface and at the center of OSB, MDF, and LVL samples during pressurization at three rates.*

	t_{Vessel} (°C)		t Surface (°C)		t_{Center} (°C)	
Samples	MIN	MAX	MIN	MAX	MIN	MAX
OSB[a]						
1.03	33.7 (6.9)	50.5 (2.9)	35.1 (2.8)	48.6 (1.6)	40.1 (3.4)	49.7 (1.8)
1.79	5.2 (7.5)	47.3 (2.8)	10.9 (6.4)	45.4 (1.3)	28.4 (11.2)	45.8 (1.8)
5.86	−7.2 (9.6)	46.4 (4.2)	14.0 (11.7)	43.5 (4.7)	29.7 (7.3)	44.2 (3.2)
MDF[b]						
1.03	34.8 (0.5)	48.1 (2.0)	25.8 (8.7)	46.2 (0.7)	40.3 (0.5)	47.3 (0.5)
1.79	−9.0 (18.5)	46.5 (3.5)	13.5 (20.1)	45.1 (2.6)	27.7 (15.7)	45.34 (1.8)
5.86	7.5 (15.0)	44.8 (2.4)	23.7 (9.1)	43.5 (0.9)	40.0 (0)	50.8 (1.2)
LVL[b]						
1.03	30.8 (3.8)	48.8 (1.2)	25.6 (7.8)	45.5 (1.2)	34.6 (5.2)	46.9 (2.5)
1.79	0.4 (6.7)	46.8 (3.6)	14.2 (8.3)	43.9 (1.9)	26.7 (6.1)	44.6 (0.3)
5.86	−1.9 (24.2)	45.4 (2.9)	18.8 (13.4)	43.0 (1.5)	26.7 (0.6)	42.7 (1.0)

[a] Averages (standard deviations) of 5 treatment runs.
[b] Averages (standard deviations) of 4 treatment runs.

TABLE 6. *Average temperature minima measured inside the treatment vessel, on the surface and at the center of OSB, MDF, and LVL samples during ventilation at three different rates.*

	Venting rate (MPa/min)	t_{Vessel} (°C) MIN	$t_{Surface}$ (°C) MIN	t_{Center} (°C) MIN
	1.03	24.6 (3.5)	22.5 (0.7)	21.5 (1.2)
OSB[a]	1.79	19.9 (2.1)	17.8 (1.3)	16.3 (1.2)
	5.86	−1.7 (2.2)	5.0 (3.2)	10.9 (1.4)
	1.03	24.7 (2.0)	24.8 (1.1)	23.5 (1.6)
MDF[a]	1.79	15.4 (0.9)	17.7 (3.4)	17.5 (0.9)
	5.86	−4.4 (0.4)	10.2 (1.7)	18.0 (1.1)
	1.03	26.4 (2.2)	23.7 (1.1)	22.2 (0.3)
LVL[b]	1.79	19.9 (1.9)	20.4 (3.2)	17.5 (1.3)
	5.86	1.5 (0.6)	7.7 (2.9)	17.3 (1.1)

[a] Averages (standard deviation) of 5 treatment runs.
[b] Averages (standard deviation) of 4 treatment runs.

cilitated more rapid temperature changes in the supercritical region, where thermal conductivity of CO_2 substantially increases (Vesovic et al. 1990). Temperature variations between the three measurement points tended to be small near or above supercritical conditions. Treatments of samples that had been stored below 0°C before the experiments showed that even temperature distribution was reached more rapidly after the system was completely filled with SC-CO_2. Differences in structural composition of the test materials were not associated with appreciable differences in temperature development, although differences in mass and heat capacity between samples produced some internal temperature differences (Table 5).

Expansion of supercritical and gaseous CO_2 during venting led to instantaneous temperature drops that were more severe at higher ventilation rates (Table 6, Fig. 19). Differences between vessel, surface, and internal temperature differed only slightly until the pressure decreased to about 4–6 MPa; then temperatures started to differ significantly from the surface. Further internal temperature decreases were dampened by the latent heat in the sample. Internal temperature continued to decline at the end of venting, even while the surface and vessel temperatures increased rapidly in response to externally applied heat. This anomaly probably reflects the continued expansion of CO_2 within the samples, especially with LVL and Douglas-fir. As with temperature decreases during pressurization, changes during venting can dramatically affect SCF solubility, and thus deposition patterns of solubilized biocides. Developing a better understanding of these changes can help in developing better processes for using both temperature and pressure to control deposition.

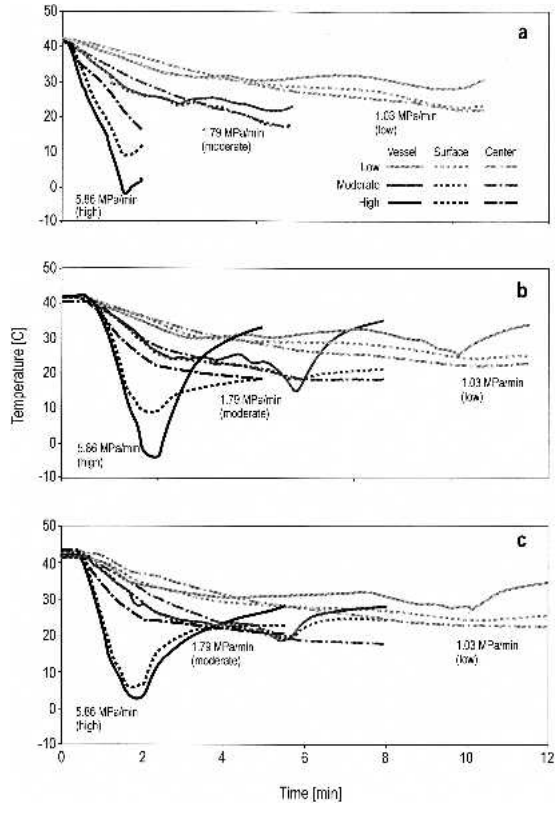

FIG. 19. Temperatures in the treatment vessel, on the surface and at the center of (a) OSB, (b) MDF, and (c) LVL samples during ventilation at 3 rates.

CONCLUSIONS

The results demonstrate that changes in wood condition following SCF impregnation can be directly linked to pressure differentials that develop during various stages of treatment. These differentials are highly dependent on material characteristics and appear to be controllable by varying process conditions to allow for adequate time for pressure equilibration. These results also suggest that careful characterization of the material properties of the wood based material can play an important role in reducing treatment damage.

ACKNOWLEDGMENTS

This is paper 3612 of the Forest Research Laboratory, Oregon State University, Corvallis, OR.

REFERENCES

ACDA, M. N., J. J. MORRELL, AND K. L. LEVIEN. 1997a. Effects of supercritical fluid treatments on physical and mechanical properties of wood-based composites. Wood Fiber Sci. 29(2):121–130.

———, ———, AND ———. 1997b. Effects of process variables on supercritical fluid impregnation of composites with tebuconazole. Wood Fiber Sci. 29(3):282–290.

———, ———, AND ———. 2001. Supercritical fluid impregnation of selected wood species with tebuconazole. Wood Sci. Technol. 35:127–136.

BEER, R., AND S. PETER. 1985. High pressure extraction of lignin from wood. Pages 385–396 *in* J. M. L. Penninger, M. Radosz, M. A. McHugh, and V. J. Krukonis, eds. Supercritical Fluid Technology. Elsevier Science Publishers B.V. Amsterdam, The Netherlands.

BERTUCCO, A., G. B. GUARISE, P. PALLADO, AND B. CORAIN. 1994. Solute deposition in a porous polymer matrix from rapid expansion of a supercritical solvent. Chem. Biochem. Eng. Q. 8(1):11–16.

BRANDT, A. C., C. PERRE, A. BEZIAT, AND M. CARLES. 1994. Neutralization and strengthening of papers with supercritical CO_2. Pages 19–24 *in* Proc. 3rd Int. Symposium on Supercritical Fluids. (Tome 2). Strasbourg, France.

CALIMLI, A., AND A. OLCAY. 1978. Supercritical-gas extraction of spruce wood. Holzforschung 32:7–10.

CHOU, Y. T. 1987. Supercritical ammonia pretreatment of lignocellulosic material. Biotech. Bioeng. Symp. 17:19–32

CHOONG, E. T., P. J. FOGG, AND F. O. TESORO. 1972. Relationship of fluid flow to treatability of wood with creosote and copper sulfate. Proc. Am. Wood-Preserv. Assoc. 68:235–249.

CLIFFORD, T. 1998. Fundamentals of supercritical fluids. Oxford Science Publications, Oxford. UK. 210 pp.

COBHAM, P., AND P. VINDEN. 1995. Internal pressure monitoring during the treatment of *Pinus radiata* (D. Don.). Int. Res. Group Wood Preserv. Doc. No. IRG/WP 95–40049. Stockholm, Sweden.

COMSTOCK, G. L. 1970. Directional permeability of softwoods. Wood Fiber 1(4):283–289.

DEBENEDETTI, P. G., AND R. C. REID. 1986. Diffusion and mass transfer in supercritical fluids. AIChE J. 32(12): 2034–2046.

ELLER, F. J., AND J. W. KING. 2000. Evaluation of critical fluid extraction and reaction of components in cedar wood. Proc. 5th International Symposium on Supercritical Fluids, Atlanta, GA, 9 p.

FREMONT, H. A. 1981. Extraction of coniferous wood with fluid CO_2 or other supercritical fluids. U.S. patent US 4,308,200.

FUNAZUKURI, T. 2000. Rates of weight loss of lignocellulosic materials subjected to supercritical fluid/mixtures. J. Chem. Eng. Japan. 33(2):292–296.

HAWES, R. I. 1996. Darcy's Law. *In* G. F. Hewitt, G. L. Shires, and Y. V. Polezhaev, eds. International encyclopedia of heat and mass transfer. CRC Press, Boca Raton, FL.

HENDRIKSEN, O. 2000. A method of performing an impregnating or extracting treatment on a resin-containing wood substrate. IPO patent WO 0,027,547.

KAMKE, F. A., AND L. J. CASEY. 1988. Gas pressure and temperature in the mat during flakeboard manufacture. Forest Prod. J. 38(3):41–43.

KAYIHAN, F. 1992. Method of perfusing a porous workpiece with a chemical compositions using cosolvents. U.S. patent US 5,094,892.

KIRAN, E. 1995. Supercritical fluid processing in the pulp and paper and forest products industry. *In* K. W. Hutchenson and N. R. Foster, eds. Innovations in supercritical fluids, ACS symposium series 608. American Chemical Society, Washington, DC. 380 pp.

LARSEN, A., N. JENTOFT, AND T GREIBROKK. 1992. Extraction of formaldehyde from particleboard with supercritical carbon dioxide. Forest Prod. J. 42(4):45–48.

LEVIEN, K. L., J. J. MORRELL, S. KUMAR, AND E. SAHLE DEMESSIE. 1994. Process for removing chemical preservatives from wood using supercritical fluid extraction U.S. patent US 5,364,475.

LOWERY, D. P. 1971. Measurement of vapor pressure generated in wood during drying. Wood Sci. 3(4):218–219.

LOWERY, D. P. 1972. Vapor pressures generated in wood during drying. Wood Sci. 5(1):73–80.

MORITA, S., T. YAMADA, AND T. HIDAKA. 1995. Supercritical fluid extraction of oxygen containing sesquiterpenes from Yakusugi (*Cryptomeria japonica*) wood. Mokuzai Gakkaishi 41(2):237–241.

MORRELL, J. J., AND K. L. LEVIEN. 2000. The deposition of a

biocide in wood-based material. Pages 227–233 *in* J. R. Williams and A. A. Clifford, eds. Methods in Biotechnology, Vol 13: Supercritical Fluid Methods and Protocols, Humana Press, Totowa, NJ.

———, ———, E. SAHLE DEMESSIE, S. KUMAR, S. SMITH, AND H. M. BARNES. 1993. Treatment of wood using supercritical fluid process. Pages 6–35 *in* Proc. 14th. Annual Meeting of Canad. Wood Preservation Assoc., Vancouver, BC.

OHIRA, T., F. TERAUCHI, AND M. YATAGAI. 1994. Tropolones extracted from the wood of western redcedar by supercritical carbon dioxide. Holzforschung 48:308–312.

ORFILA, C., AND J. P. HOSLI. 1985. Pressure development in low permeable woods during the intrusion of air. Proc. Annual Meeting of American Wood-Preservers' Assoc. 81:111–125.

PING, Z. 1997. Removal of copper from chromated copper arsenate treated wood with supercritical carbon dioxide. M.S. thesis, Michigan Technological Univ., Houghton, MI. 77 pp.

RESCH, H., AND D. G. ARGANBRIGHT. 1970. Application of electrical transducers to research in wood preservation. Forest Prod. J. 20(6):23–26.

RITTER, D. C., AND A. G. CAMPBELL. 1986. The effect of supercritical carbon dioxide extraction on pine wood structure. Pages 179–182 *in* Proc. 8th Symposium on Biotechnology for Fuels and Chemicals. J. Wiley, New York, NY.

———, AND ———. 1991. Supercritical carbon dioxide extraction of southern pine and ponderosa pine. Wood Fiber Sci. 23(1):98–113.

RUDDICK, J. N. R., AND F. CUI. 1995. Extraction of toxic organic contaminants from wood and photodegradation of toxic organic contaminants. U.S. patent US 5476975.

SAHLE DEMESSIE, E. 1994. Deposition of chemicals in semiporous solids using supercritical fluid carriers. Ph.D. dissertation, Oregon State Univ., Corvallis, OR. 301 pp.

———, A. HASSAN, K. L. LEVIEN, S. KUMAR, AND J. J. MORRELL. 1995. Supercritical carbon dioxide treatment: Effect on permeability of Douglas-fir heartwood. Wood Fiber Sci. 27(3):296–300.

———, K. L. LEVIEN, AND J. J. MORRELL. 1998. Impregnating porous solids using supercritical CO_2. Chemtech. 28(3):12–18.

———, J. S. YI, K. L. LEVIEN, AND J. J. MORRELL. 1997. Supercritical fluid extraction of pentachlorophenol from pressure-treated wood. Sep. Sci. 32(6):1067–1085.

SCHNEIDER, P. F. 1999. Pressure measurement in wood as a method to understand pressure impregnation processes: Bethell, Rueping, Lowry, and supercritical carbon dioxide. Ph.D. dissertation, Oregon State Univ., Corvallis, OR. 243 pp.

———, AND J. J. MORRELL. 1997. Internal pressure development in Douglas-fir during pressure treatment. Int. Res. Group on Wood Pres. Doc. No. IRG/WP 97–40091. Stockholm, Sweden. 7 p.

SMITH, S. M., E. S. DEMESSIE, J. J. MORRELL, K. LEVIEN, AND H. NG. 1993. Supercritical fluid (SCF) treatment: its effect on the bending strength of ponderosa pine sapwood. Wood Fiber Sci. 25:119–123.

SUNOL, A. K. 1991. Supercritical fluid aided treatment of porous material, U.S. patent US 4,992,308.

———. 1992. Supercritical fluid aided treatment of porous material, U.S. patent US 5,169,687.

TERAUCHI, F., T. OHIRA, M. YATAGI, T. OHGAMA, H. AOKI, AND T. SUZUKI. 1993. Extraction of volatile compounds from coniferous woods with supercritical carbon dioxide. Mokuzai Gakkaishi 39(12):1421–1430.

U.S. DEPARTMENT OF AGRICULTURE (USDA). 1999. Wood Handbook: Wood as an Engineering Material. USDA General Technical Report FPL-GTR-113. U.S. Forest Products Laboratory, Madison, WI. 463 pp.

VESOVIC, V., W. A. WAKEHAM, G. A. OLCHOWY, J. V. SENGERS, J. T. R. WATSON, AND J. MILLAT. 1990. The transport properties of carbon dioxide. J. Phys. Chem. Ref. Data 19(3):763–808.

ZAVALA, D. 1990. The hot pressing of veneer-based composites. Ph.D. dissertation, Oregon State Univ., Corvallis, OR. 201 pp.

———, AND P. E. HUMPHREY. 1996. Hot pressing veneer-based products: The interaction of physical process. Forest Prod. J. 46(1):69–77.